THE JOURNAL OF BIOLOGICAL CHEMISTRY VOL. 280, NO. 49, pp. 40500–40508, December 9, 2005

The AraC-type Regulator RipA Represses Aconitase and Other Iron Proteins from *Corynebacterium* under Iron Limitation and Is Itself Repressed by DtxR*[S]

Received for publication, August 8, 2005, and in revised form, September 22, 2005 Published, JBC Papers in Press, September 22, 2005, DOI 10.1074/jbc.M508693200

Julia Wennerhold[1], **Andreas Krug**[1], **and Michael Bott**[2]

From the Institut für Biotechnologie 1, Forschungszentrum Jülich, Jülich D-52425, Germany

The mRNA level of the aconitase gene *acn* of *Corynebacterium glutamicum* is reduced under iron limitation. Here we show that an AraC-type regulator, termed RipA for "regulator of iron proteins A," is involved in this type of regulation. A *C. glutamicum* Δ*ripA* mutant has a 2-fold higher aconitase activity than the wild type under iron limitation, but not under iron excess. Comparison of the mRNA profiles of the Δ*ripA* mutant and the wild type revealed that the *acn* mRNA level was increased in the Δ*ripA* mutant under iron limitation, but not under iron excess, indicating a repressor function of RipA. Besides *acn*, some other genes showed increased mRNA levels in the Δ*ripA* mutant under iron starvation (*i.e.* those encoding succinate dehydrogenase (*sdhCAB*), nitrate/nitrite transporter and nitrate reductase (*narKGHJI*), isopropylmalate dehydratase (*leuCD*), catechol 1,2-dioxygenase (*catA*), and phosphotransacetylase (*pta*)). Most of these proteins contain iron. Purified RipA binds to the upstream regions of all operons mentioned above and in addition to that of the catalase gene (*katA*). From 13 identified binding sites, the RipA consensus binding motif RRGCGN$_4$RYGAC was deduced. Expression of *ripA* itself is repressed under iron excess by DtxR, since purified DtxR binds to a well conserved binding site upstream of *ripA*. Thus, repression of *acn* and the other target genes indicated above under iron limitation involves a regulatory cascade of two repressors, DtxR and its target RipA. The modulation of the intracellular iron usage by RipA supplements mechanisms for iron acquisition that are directly regulated by DtxR.

Corynebacterium glutamicum is a nonpathogenic, aerobic Gram-positive soil bacterium that is used for large scale industrial production of amino acids, predominantly L-glutamate (1.5 million tons/year) and L-lysine (0.7 million tons/year). In addition, *C. glutamicum* has gained interest as a suitable model organism for the *Corynebacterineae*, a suborder of the actinomycetes that includes the genus *Mycobacterium*. An overview on *C. glutamicum* biology, genetics, physiology, and biotechnology can be found in a recent monograph (1).

The citric acid cycle is of central importance for metabolism in general and for amino acid production in particular, because it provides the biosynthetic precursors of the aspartate and glutamate family of amino acids. Despite its key role, knowledge about the genetic regulation of this pathway in *C. glutamicum* is scarce. We recently could show that the activity of aconitase (EC 4.2.1.3), which catalyzes the stereospecific and reversible isomerization of citrate to isocitrate via *cis*-aconitate, varies depending on the carbon source and that this is caused by transcriptional regulation (2). A repressor of the TetR family, called AcnR, was identified, which represses aconitase by binding to an imperfect inverted repeat within the *acn* promoter region and interfering with the binding of RNA polymerase (2). The factors that control binding of AcnR to its operator are not yet known. DNA microarray experiments revealed that *acn* expression is not only influenced by the carbon source but also by the iron concentration of the medium (2). Under iron limitation, the *acn* mRNA level in the wild type was 3-fold lower than under iron excess. In the Δ*acnR* mutant, this decrease was even larger (4.8-fold), presumably because the increased expression of aconitase, which contains a 4Fe-4S cluster, leads to an enhanced iron starvation.

We now have identified a new transcriptional regulator, designated RipA, which is responsible for iron-dependent regulation of aconitase and several other iron-containing proteins. Evidence is provided that RipA represses *acn* and six other target operons under iron limitation and is itself repressed under iron excess by the global iron repressor DtxR.

EXPERIMENTAL PROCEDURES

Bacterial Strains, Media, and Growth Conditions—All strains and plasmids used in this work are listed in supplemental Table S1. The *C. glutamicum* type strain ATCC13032 (3) was used as wild type. Strain Δ*ripA* is a derivative containing an in-frame deletion of the *ripA* gene. For growth experiments, 5 ml of brain heart infusion medium (Difco) was inoculated with colonies from a fresh LB agar plate (4) and incubated for 6 h at 30 °C. After washing, the cells of this first preculture were used to inoculate a 500-ml shake flask containing 50 ml of CGXII minimal medium (5) with 4% (w/v) glucose and either 1 μM $FeSO_4$ (iron starvation) or 100 μM $FeSO_4$ (iron excess). This second preculture was cultivated overnight at 30 °C and then used to inoculate the main culture to an A_{600} ~1. The main culture contained the same iron concentration as the second preculture. The trace element solution with iron salts omitted and the $FeSO_4$ solution were always added after autoclaving. For growth of *C. glutamicum* strains carrying plasmid pJC1 or pJC1-*ripA*, the medium was supplemented with 25 μg/ml kanamycin. For all cloning purposes, *Escherichia coli* DH5 (Invitrogen) was used as host, for overproduction of RipA and DtxR *E. coli* BL21(DE3) (6). The *E. coli* strains were cultivated aerobically in LB medium at 37 °C (DH5) or at 30 °C (BL21(DE3)). When appropriate, kanamycin was added to a concentration of 50 μg/ml.

Recombinant DNA Work—The enzymes for recombinant DNA work were obtained from Roche Applied Science or New England Biolabs (Frankfurt, Germany). The oligonucleotides used in this study were obtained from Operon (Cologne, Germany) and are listed in supplemental Table S2. Routine methods like PCR, restriction, or ligation were

* The costs of publication of this article were defrayed in part by the payment of page charges. This article must therefore be hereby marked "*advertisement*" in accordance with 18 U.S.C. Section 1734 solely to indicate this fact.
[S] The on-line version of this article (available at http://www.jbc.org) contains supplemental Tables S1 and S2 and supplemental Figs. S1 and S2.
[1] Both authors contributed equally to this work.
[2] To whom correspondence should be addressed. Tel.: 49-2461-615515; Fax: 49-2461-612710; E-mail: m.bott@fz-juelich.de.

carried out according to standard protocols (4). Chromosomal DNA from *C. glutamicum* was prepared as described (7). Plasmids from *E. coli* were isolated with the QIAprep spin miniprep kit (Qiagen, Hilden, Germany). *E. coli* was transformed by the RbCl method (8), and *C. glutamicum* was transformed by electroporation (9). DNA sequencing was performed with a Genetic Analyzer 3100-Avant (Applied Biosystems, Darmstadt, Germany). Sequencing reactions were carried out with the Thermo Sequenase primer cycle sequencing kit (Amersham Biosciences).

An in-frame *ripA* deletion mutant of *C. glutamicum* was constructed via a two-step homologous recombination procedure as described previously (10). The *ripA* up- and downstream regions (~500 bp each) were amplified using the oligonucleotide pairs orf1558-A-for/orf1558-B-rev and orf1558-C-for/orf1558-D-rev, respectively, and the products served as template for cross-over PCR with oligonucleotides orf1558-A-for and orf1558-D-rev. The resulting PCR product of ~1 kb was digested with EcoRI and HindIII and cloned into pK19*mobsacB* (11). DNA sequence analysis confirmed that the cloned PCR product did not contain spurious mutations. Transfer of the resulting plasmid pK19*mobsacB*-Δ*ripA* into *C. glutamicum* and screening for the first and second recombination event were performed as described previously (10). Kanamycin-sensitive and saccharose-resistant clones were tested by PCR analysis of chromosomal DNA with the primer pair orf1558-amp-for/orf1558-amp-rev (supplemental Table S2). Of 10 clones tested, five showed the wild-type situation (2.0-kb fragment) and five had the desired in-frame deletion of the *ripA* gene (1.1-kb fragment), in which all nucleotides except for the first six codons and the last 12 codons were replaced by a 21-bp tag.

In order to complement the Δ*ripA* mutant, the *ripA* coding region and 250-bp upstream DNA containing the promoter region were amplified using oligonucleotides (ripA+250-for (2) and ripA+250-rev) introducing a SalI and a PstI restriction site, respectively. The resulting 1245-bp PCR product was cloned into the vector pJC1 (12). The resulting plasmid pJC1-ripA and pJC1 were used to transform *C. glutamicum* wild type and the Δ*ripA* strain.

For overproduction and purification of RipA with an N-terminal StrepTag-II (13), the *ripA* coding region was amplified using oligonucleotides that introduce an NdeI restriction site, including the start codon (ripA-2-for) and an XhoI restriction site after the stop codon (ripA-2-rev). The purified PCR product was cloned in the modified expression vector pET28b-Streptag (14), resulting in plasmid pET28b-Streptag-*ripA*. The RipA protein encoded by this plasmid contains 14 additional amino acids (MASWSHPQFEKGAH) at the amino terminus. For overproduction and purification of DtxR, the *dtxR* coding region (equivalent to NCgl1845) was amplified using oligonucleotides that introduced an NdeI restriction site at the translation initiation codon (dtxR-for-1) and four histidine codons plus an XhoI restriction site before the stop codon (dtxR-rev-1). The PCR product was cloned into the pET24b vector, resulting in plasmid pET24b-*dtxR*-C. The DtxR protein encoded by this plasmid contains 12 additional amino acids at the carboxyl terminus (HHHHLEHHHHHH). The PCR-derived portions of pET28b-Streptag-*ripA* and pET24b-*dtxR*-C were analyzed by DNA sequence analysis and found to contain no spurious mutations. For overproduction of RipA and DtxR, the two plasmids were transferred into *E. coli* BL21(DE3).

Preparation of Total RNA—Cultures of the wild type and the Δ*ripA* mutant were grown in CGXII minimal medium containing 4% (w/v) glucose under iron limitation (1 μM $FeSO_4$) or iron excess (100 μM $FeSO_4$). In the exponential growth phase at an A_{600} of 4–6, 25 ml of the cultures were used for the preparation of total RNA as described previously (15). Isolated RNA samples were analyzed for quantity and quality by UV spectrophotometry and denaturing formaldehyde-agarose gel electrophoresis (4), respectively, and stored at −70 °C until use.

DNA Microarray Analyses—The generation of whole-genome DNA microarrays (16), synthesis of fluorescently labeled cDNA from total RNA, microarray hybridization, washing, and data analysis were performed as described previously (2, 17–19). Genes that exhibited significantly changed mRNA levels ($p < 0.05$ in a Student's t test) by at least a factor of 1.7 were determined in two series of DNA microarray experiments: (i) five comparisons of the wild type and the Δ*ripA* mutant cultivated in CGXII minimal medium with 4% (w/v) glucose under iron limitation (1 mM $FeSO_4$); (ii) two comparisons of the wild type and the Δ*ripA* mutant cultivated in CGXII-glucose medium under iron excess (100 μM $FeSO_4$).

Aconitase Assay—Aconitase activity was determined as the rate of *cis*-aconitate formation from isocitrate (20), as described previously (2), except that the assay was performed at 30 °C. Cells of the 20-ml main culture were harvested by centrifugation at 5,000 × *g* for 10 min and 4 °C. The cell pellet was resuspended in 90 mM Tris/HCl, pH 8.0, and used for the preparation of cell extract. The assay mixture contained 950–995 μl of 90 mM Tris/HCl, pH 8.0, and 20 mM DL-trisodium isocitrate. The reaction was started with the addition of 5–50 μl of cell extract, and the formation of *cis*-aconitate was followed by measuring the absorbance increase at 240 nm using a Jasco V560 spectrophotometer. An extinction coefficient for *cis*-aconitate of 3.6 mM^{-1} cm^{-1} at 240 nm was used. One unit of activity corresponds to 1 μmol of isocitrate converted to *cis*-aconitate per min.

Overproduction and Purification of RipA—E. coli BL21(DE3) carrying the plasmid pET28b-*strep-ripA* was grown at 30 °C in 200 ml of LB medium with 50 μg/ml kanamycin to an A_{600} of ~1.2 before adding 1 mM isopropyl β-D-thiogalactoside. After cultivation for another 4 h, cells were harvested by centrifugation, washed once, and stored at −20 °C. For cell extract preparation, thawed cells were resuspended in 10 ml of buffer W (100 mM Tris/HCl, pH 8.0, 150 mM NaCl). After the addition of 1 mM diisopropylfluorophosphate and 1 mM phenylmethylsulfonyl fluoride, the cell suspension was passed three times through a French pressure cell (SLM Aminco, Spectronic Instruments, Rochester, NY) at 207 megapascals. Intact cells and cell debris were removed by centrifugation (15 min, 5,000 × *g*, 4 °C), and the cell-free extract was subjected to ultracentrifugation (1 h, 150,000 × *g*, 4 °C). The supernatant obtained after ultracentrifugation was applied to a StrepTactin-Sepharose column with a bed volume of 1 ml (IBA, Göttingen, Germany). The column was washed with 6 ml of buffer W, and RipA tagged with StrepTag-II was eluted with 8 × 0.5 ml of buffer W containing 7.5 mM desthiobiotin (Sigma). Fractions containing RipA were pooled, and the buffer was exchanged against TG buffer (30 mM Tris/HCl, pH 7.5, 10% (v/v) glycerin) using Vivaspin concentrators with a cut-off of 10 kDa. Protein concentrations were determined with the BCA protein assay kit (Pierce) using bovine serum albumin as a standard. The purity of the protein preparations was assessed by SDS-PAGE and subsequent protein detection with Gel Code blue stain reagent (Pierce). Using this protocol, ~0.2 mg of RipA protein was purified to apparent homogeneity from 200 ml of culture.

Overproduction and Purification of DtxR—E. coli BL21(DE3) carrying the plasmid pET24b-*dtxR* was grown at 30 °C in 100 ml of LB with 50 μg/ml kanamycin. Expression was induced at an A_{600} of ~0.3 with 1 mM isopropyl β-D-thiogalactoside. Four hours after induction, cells were harvested by centrifugation and stored at −20 °C. For cell extract preparation, thawed cells were washed once and resuspended in 10 ml of TNGI5 buffer (20 mM Tris/HCl, pH 7.9, 300 mM NaCl, 5% (v/v) glycerol,

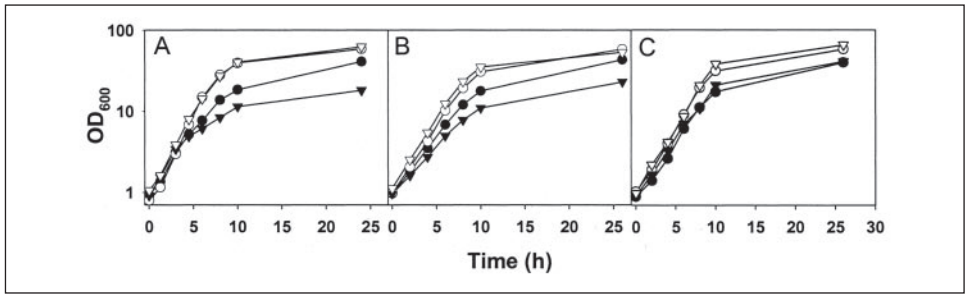

FIGURE 1. **Growth of *C. glutamicum* wild type (*circles*) and the Δ*ripA* mutant (*triangles*) in CGXII minimal medium with 4% (w/v) glucose and either 100 μM $FeSO_4$ (*open symbols*) or 1 μM $FeSO_4$ (*filled symbols*).** In the experiments shown in *A–C*, the strains contained either no plasmid (*A*) or pJC1 (*B*) or pJC1-*ripA* (*C*).

5 mM imidazol) containing 1 mM diisopropylfluorophosphate and 1 mM phenylmethylsulfonyl fluoride. Disruption of the cells and fractionation by centrifugation was performed as described above for RipA purification. DtxR present in the supernatant of the ultracentrifugation step was purified by nickel affinity chromatography using nickel-activated nitrilotriacetic acid-agarose (Novagen). After washing the column with TNGI50 buffer (which contains 50 mM imidazol), DtxR protein was eluted with TNGI100 buffer (which contains 100 mM imidazol). Fractions containing DtxR were pooled, and the elution buffer was exchanged against TG buffer (30 mM Tris/HCl, pH 7.5, 10% (v/v) glycerin). From 100 ml of culture, ~3 mg of DtxR was purified to apparent homogeneity.

Gel Shift Assays—For band shift assays of RipA with putative target promoters, purified RipA protein was mixed with DNA fragments (200–630 bp, final concentration 8–13 nM) in a total volume of 20 μl. The binding buffer contained 20 mM Tris/HCl, pH 7.5, 0.5 mM EDTA, 5% (v/v) glycerol, 1 mM dithiothreitol, 0.005% (v/v) Triton X-100, 50 mM NaCl, 5 mM $MgCl_2$, and 2.5 mM $CaCl_2$. Approximately 20 nM of different nontarget promoter fragments (*clpC*, *clpP*, *ripA*, and *porB*) were added as a negative control. After incubation for 30 min at room temperature, the samples were separated on a 10% native polyacrylamide gel at room temperature and 170 V using 1× TBE (89 mM Tris base, 89 mM boric acid, 2 mM EDTA) as electrophoresis buffer. The gels were subsequently stained with Sybr Green I according to the instructions of the supplier (Sigma) and photographed.

Binding of DtxR to the *ripA* promoter was carried out in a 20-μl reaction mixture containing 100 mM Tris/HCl (pH 7.5), 5 mM $MgCl_2$, 40 mM KCl, 10% (v/v) glycerol, 1 mM dithiothreitol, 150 μM $MnCl_2$, an 18 nM concentration of a 300-bp *ripA* promoter DNA fragment, and DtxR in concentrations ranging from 0 to 3.6 μM. The *ripA* fragment covered the region from position −230 to +70 relative to the translation start and was obtained by PCR with primers ripA-Prom-for and ripA-Prom-rev. As a negative control, a 23 nM concentration of a 200-bp *acn* promoter fragment extending from position +190 to −50 relative to the *acn* transcription start site (2) was added. This fragment was amplified with primers acn-Prom4-for and acn-Prom4-rev. The reaction mixture was incubated at room temperature for 30 min and then loaded onto a 10% native polyacrylamide gel containing 1 mM dithiothreitol and 150 μM $MnCl_2$. Electrophoresis was performed at room temperature and 170 V using 1× TB (89 mM Tris base, 89 mM boric acid) supplemented with 1 mM dithiothreitol and 150 μM $MnCl_2$ as electrophoresis buffer. All PCR products used in the gel shift assays were purified with the PCR purification Kit (Qiagen, Hilden, Germany) and eluted in EB buffer (10 mM Tris/HCl, pH 8.5).

RESULTS

Identification of RipA as a Potential Iron-dependent Regulator of the Aconitase Gene—In a previous study, we showed that expression of the aconitase gene *acn* of *C. glutamicum* is influenced by the iron availability, being reduced under iron limitation (2). This regulation also occurred in a mutant lacking AcnR, a repressor of the *acn* gene, and thus must be mediated by a different regulator or regulatory mechanism. A candidate gene that might be responsible for iron-dependent regulation of *acn* was identified in the DNA microarray experiments used to compare the gene expression profile of *C. glutamicum* under iron excess and iron limitation. Expression of the gene NCgl0943 was strongly influenced by the iron availability (2). Its mRNA level was always found to be increased under iron-limiting conditions, and it thus behaved like typical iron starvation genes. The protein derived from NCgl0943 is composed of 331 amino acid residues (36.044 kDa) and contains a DNA binding domain of the AraC family (PF00165 in the PFAM data base (21), PS01124 in the PROSITE data base (22)) with two helix-turn-helix motifs extending from position 113 to 159 and from position 165 to 208. It is flanked by amino- and carboxyl-terminal domains of 112 and 123 residues, respectively, which show no significant sequence similarity to other proteins. Based on the results described below, the NCgl0943 gene was designated *ripA* (repressor of iron proteins A).

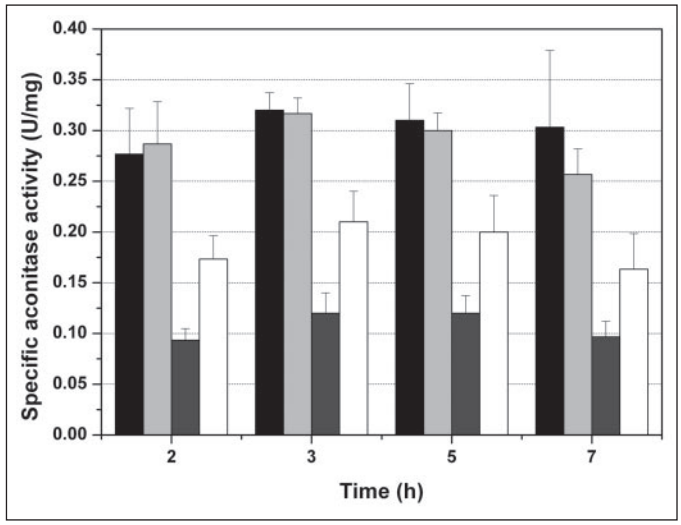

FIGURE 2. **Aconitase activity of *C. glutamicum* wild type and the Δ*ripA* mutant cultivated under iron excess (100 μM $FeSO_4$) and iron limitation (1 μM $FeSO_4$).** Cells were grown in CGXII minimal medium with 4% (w/v) glucose and harvested at four time points within the exponential growth phase (A_{600} between 2 and 9). Aconitase activity was determined in cell-free extracts. *Black* and *dark gray bars*, wild type cultivated with 100 μM iron and 1 μM iron, respectively. *Light gray bars* and *white bars*, Δ*ripA* cultivated with 100 μM iron and 1 μM iron, respectively. The values for the specific activity represent means ± S.D. for at least three independent cultivations and two determinations per experiment.

In order to test an involvement of the RipA protein in *acn* regulation, a *ripA* deletion mutant of *C. glutamicum* was constructed. In a first set of experiments, the growth behavior of the Δ*ripA* mutant was tested. As shown in Fig. 1*A*, no differences were observed between wild type and mutant cultivated in glucose minimal medium containing excess iron

TABLE ONE

Genes showing altered expression in the *C. glutamicum* Δ*ripA* mutant compared with wild type

NCgl number[a]	Gene	Annotation	Ratio, iron limitation[a]	Ratio, iron excitation[b]
NCgl2319	*catA*	Catechol 1,2-dioxygenase	4.41	1.03
NCgl1482	*acn*	Aconitase	2.40	0.88
NCgl1262	*leuC*	3-Isopropylmalate dehydratase, large subunit	1.65	0.90
NCgl1263	*leuD*	3-Isopropylmalate dehydratase, small subunit	2.13	0.91
NCgl0359	*sdhC*	Succinate dehydrogenase, cytochrome *b* subunit	1.90	0.85
NCgl0360	*sdhA*	Succinate dehydrogenase, flavoprotein	1.71	0.81
NCgl0361	*sdhB*	Succinate dehydrogenase, FeS protein	1.64	1.01
NCgl1143	*narK*	Nitrate/nitrite transporter	1.63	1.04
NCgl1142	*narG*	Nitrate reductase, α subunit	1.89	1.00
NCgl1141	*narH*	Nitrate reductase, β subunit	1.67	0.90
NCgl1140	*narJ*	Nitrate reductase, δ subunit	1.75	1.05
NCgl1139	*narI*	Nitrate reductase, γ subunit	1.72	0.99
NCgl2657	*pta*	Phosphotransacetylase	1.82	1.24
NCgl2439	*ftn*	Ferritin	0.55	0.58
NCgl1490		Putative membrane protein	0.52	0.65
NCgl2434		Putative membrane protein	0.46	0.91
NCgl0140		Putative sugar *O*-acetyltransferase	0.44	1.09
NCgl1096		Putative flavin-containing monooxygenase	0.38	0.46
NCgl2001		Conserved hypothetical protein	0.30	0.81
NCgl2897	*dps*	Starvation-induced DNA protection protein	0.29	0.30
NCgl0943	*ripA*	Transcriptional regulator, AraC family	0.11	0.16

[a] This column includes those genes whose average mRNA ratio (Δ*ripA* mutant/wild type) was altered ≥1.7-fold or ≤1.7-fold (p value ≤0.05) in five DNA microarray experiments performed with RNA isolated from five independent cultivations in CGXII minimal medium under iron limitation (1 μM $FeSO_4$). The genes *leuC*, *sdhB*, *narK*, and *narH* show an average mRNA ratio below 1.7 but were included, since they are organized in operons with genes (*leuD*, *sdhCA*, or *narKGJI*) having an mRNA ratio above 1.7.

[b] This column provides the mRNA ratio (Δ*ripA* mutant/wild type) of the genes under iron excess conditions. It represents the average of two DNA microarray experiments performed with RNA isolated from two independent cultivations in CGXII minimal medium under iron excess (100 μM $FeSO_4$).

(100 μM). However, under iron-limiting conditions (1 μM), the *ripA* mutant grew initially like the wild type, but after an A_{600} of about 5, the growth rate of the mutant decreased more strongly than that of the wild type. The final cell density of the mutant (A_{600} of 20) was only half that of the wild type (A_{600} = 40). Thus, the Δ*ripA* mutant has a growth defect under iron limitation but not under iron excess. As shown in Fig. 1*C*, this growth defect could be reversed by transformation with a plasmid carrying the *ripA* gene with its native promoter region (pJC1-*ripA*), but not with pJC1 alone (Fig. 1*B*).

In a second set of experiments, aconitase activity was determined in wild-type and Δ*ripA* cells from cultures grown under iron excess and iron limitation. As shown in Fig. 2, the aconitase activity of the two strains was nearly identical under iron excess, whereas under iron limitation, the Δ*ripA* mutant had a 1.5–2-fold higher activity than the wild type at four different time points. Thus, the absence of *ripA* might result in an increased expression of the *acn* gene under iron limitation, but not under iron excess.

Comparison of the Expression Profiles of Δ*ripA Mutant and Wild Type with DNA Chips*—In order to determine the effects of RipA on *acn* expression as well as on global gene expression, whole genome DNA microarrays of *C. glutamicum* (16) were used to compare the mRNA ratios of the Δ*ripA* mutant and the wild type under iron limitation and iron excess. Under iron starvation (1 μM iron), nine genes showed a >1.7-fold higher mRNA level in the Δ*ripA* mutant (TABLE ONE). This group included the aconitase gene *acn*, supporting the above made assumption that increased *acn* expression is responsible for the elevated aconitase activity in the Δ*ripA* mutant under iron limitation. Besides *acn*, *catA* (catechol 1,2-dioxygenase), *leuCD* (isopropylmalate dehydratase), *narKGHJI* (nitrate/nitrite transporter and nitrate reductase), *sdhCAB* (succinate dehydrogenase), and *pta* (phosphotransacetylase) showed higher mRNA levels in the Δ*ripA* mutant compared with the wild type. The mRNA level of the *ackA* gene for acetate kinase, which is co-transcribed with *pta* (23), was slightly increased in the Δ*ripA* mutant but below the cut-off used. Except for the transporter NarK, phosphotransacetylase, and acetate kinase, the enzymes encoded by these genes are known to contain iron, mostly in the form of iron-sulfur clusters (aconitase, isopropylmalate dehydratase, nitrate reductase, succinate dehydrogenase) and/or heme (nitrate reductase, succinate dehydrogenase) (24). Remarkably, the mRNA level of the genes mentioned above was changed only under iron limitation but not under iron excess (TABLE ONE).

Besides *ripA*, seven other genes showed a >1.7-fold decreased mRNA level in the Δ*ripA* mutant under iron limitation (TABLE ONE). There is no obvious common property of these genes; however, *dps* (starvation-induced DNA protection protein) and *ftn* (ferritin) are critically involved in iron homoeostasis (25, 26). In contrast to the genes with an increased mRNA level in the Δ*ripA* mutant, *dps* and *ftn* had decreased mRNA levels not only under iron limitation but also under iron excess.

Binding of Purified RipA Protein to the acn Promoter—In order to test whether the influence of RipA on *acn* expression is direct, binding of RipA to the *acn* promoter was analyzed. For that purpose, the RipA protein containing an amino-terminal StrepTag-II was overproduced in *E. coli* and purified to apparent homogeneity by affinity chromatography (Fig. 3). Gel shift assays showed that the RipA protein bound with high affinity to fragment 1 covering the entire *acn* promoter region, whereas a control fragment covering the promoter of the *porB* gene encoding an anion channel (27) was not shifted (Fig. 4). A RipA-fragment 1 complex was already observed at a 5-fold molar excess of RipA. At a 10-fold excess, two RipA-fragment 1 complexes were observed, and at a 30-fold excess, only the second RipA-DNA complex was observed, suggesting the presence of two binding sites. Gel shift assays with 10 different subfragments (Fig. 4) clearly confirmed the presence of two

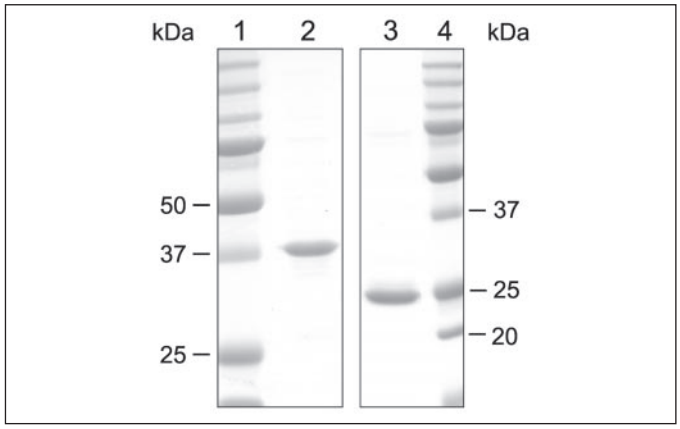

FIGURE 3. **Purification of RipA and DtxR.** *Lane 1*, protein standard; *lane 2*, purified RipA obtained after desthiobiotin elution from a StrepTactin affinity column; *lane 3*, purified DtxR obtained after imidazol elution from a nickel-chelate affinity column; *lane 4*, protein standard. Proteins were separated on a 12% SDS-polyacrylamide gel and stained with Coomassie Blue.

distinct binding sites, extending from position −212 to −194 (binding site A) and from −155 to −137 (binding site B) relative to the transcription start site of *acn* determined previously (2). Fragments lacking these regions (*e.g.* fragment 2) were not shifted, fragments containing one of the two regions formed a single RipA-DNA complex (*e.g.* fragment 7), and fragments containing both regions (*e.g.* fragment 8) formed two RipA-DNA complexes (Fig. 4).

Inspection of the two regions revealed that they contained a similar sequence motif but in opposite orientation (Fig. 5). The relevance of this motif was tested by mutational analysis, in which three or four nucleotides were exchanged simultaneously. As shown in Fig. 5, all mutations within the proposed motif prevented RipA binding, whereas the mutations outside did not inhibit binding. These results confirmed the importance of the sequence G(A/T)GCGN$_6$GAC for RipA binding.

Binding of Purified RipA Protein to Additional Target Promoters—As a result of the DNA microarray experiments, the operons *catA*, *leuCD*, *narKGHJI*, *sdhCAB*, and *pta-ack* were identified as further putative target genes of RipA, since their mRNA level was also increased in the Δ*ripA* mutant. We therefore tested the binding of RipA to the corresponding promoter regions. As shown in Fig. 6, all five promoter fragments were shifted by RipA at a molar excess (protein/DNA) of 5–10, and in all cases, two RipA-DNA complexes were formed. This indicates that there are two RipA binding sites in the corresponding promoter regions, as shown above for the *acn* promoter. Since expression of the *katA* gene encoding the hemoprotein catalase was also altered in some of the DNA microarray experiments, the *katA* promoter region was also tested for RipA binding and shown to contain two RipA binding sites with affinities comparable with those described above. In addition, a third binding site of lower affinity was detected (Fig. 6). Binding of RipA was also tested with the promoter regions of *ripA*, *dps*, and *ftn*. In the case of *ripA* and *dps*, no shift was observed, suggesting that there is no autoregulation of *ripA* and no direct control of *dps* expression by RipA. In the case of *ftn*, a weak binding was observed, with about 30% of the *ftn* fragment shifted at a 100-fold molar excess of RipA (data not shown). For the other RipA targets, a complete shift was observed at a 10–30-fold molar RipA excess. Thus, the affinity of RipA to the *ftn* promoter appears to be much lower. If RipA directly influences *ftn* expression, it should act as an activator, since the *ftn* mRNA level was decreased in the Δ*ripA* mutant. Considering that induction of an iron storage protein under iron limitation appears counterproductive, the role of RipA in *ftn* expression is not yet clear.

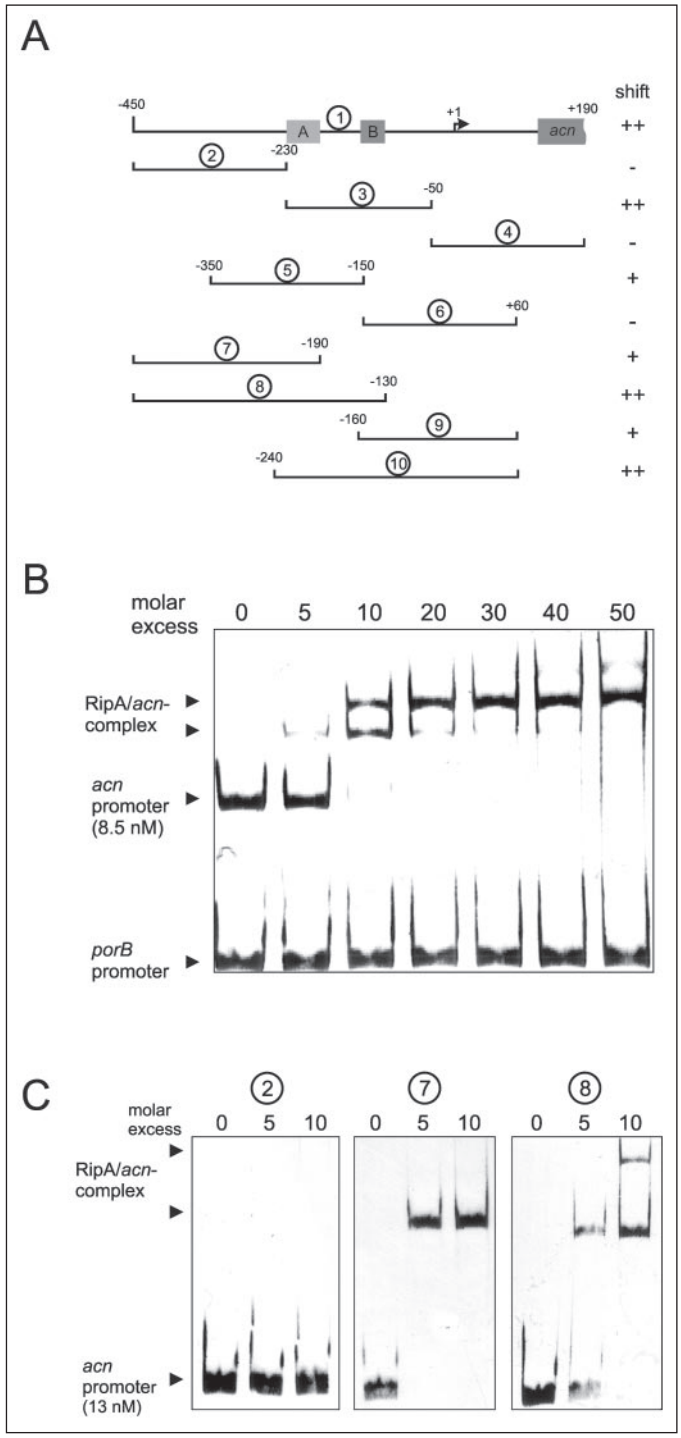

FIGURE 4. **Binding of RipA to the *acn* promoter.** *A*, DNA fragments (*circled 1–10*) used to analyze RipA binding to the *acn* promoter by gel shift assays. The *numbers* indicate the ends of the fragments relative to the *acn* transcription start site (+1). Oligonucleotides used for amplification of the 10 fragments by PCR are listed in supplemental Table S2 (acn-for-3–acn-Prom10-for). At the *right*, it is indicated whether the fragment was shifted once (+), twice (++), or not at all (−). The *boxes labeled A* and *B* indicate the regions that were identified to contain RipA binding sites. *B*, gel showing binding of purified RipA (5–50-fold molar excess) to fragment 1 (8.5 nM 632-bp fragment). A 485-bp *porB* promoter fragment (11 nM) served as negative control. The DNA-protein mixture was incubated for 30 min at room temperature before separation by native polyacrylamide gel electrophoresis (10%) and staining with SybrGreen I. *C*, gel showing binding of RipA (5- and 10-fold molar excess) to fragment 2 (no binding site), fragment 7 (one binding site), and fragment 8 (two binding sites).

As described above for *acn*, the RipA binding sites within the *sdhCAB* promoter were narrowed down with six different subfragments (data not shown). In this way, binding site A was shown to be located in the

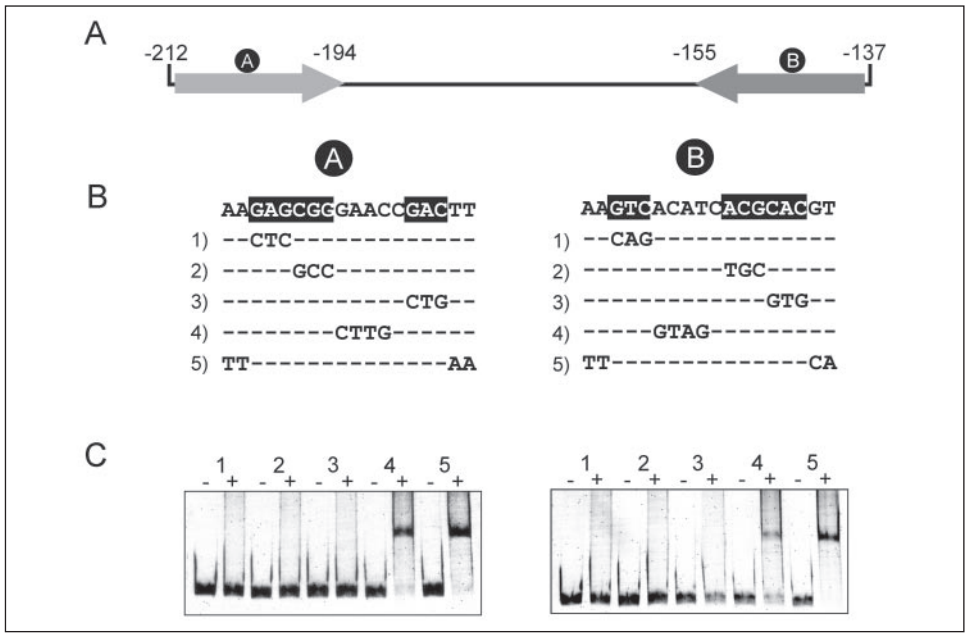

FIGURE 5. **Mutational analysis of the RipA binding sites within the *acn* promoter.** *A*, the *two inverted arrows* denoted *A* and *B* indicate the two RipA binding sites forming an imperfect inverted repeat as deduced from gel shift assays. The *numbers* indicate their positions relative to the *acn* transcription start site. *B*, mutations introduced within (*1*, *2*, and *3*) and outside (*4* and *5*) the proposed RipA binding sites A and B are listed *below* the wild-type sequence. Fragments containing these mutations were obtained with the primer pairs acn-A.1/acn-for-3 to acn-A.5/acn-for-3 and acn-B.1/acn-Prom4-rev to acn-B.5/acn-Prom4-rev (see supplemental Table S2). *C*, gel showing binding of RipA to the mutated DNA fragments. Approximately 30 nM fragments A1–A5 and B1–B5 were incubated for 30 min at room temperature either without RipA (*lanes* labeled with a *minus sign*) or with 1.2 μM of purified RipA protein (*lanes* labeled with a *plus sign*). Subsequently, the samples were separated on a 10% nondenaturating polyacrylamide gel, and the gels were stained with SybrGreen I.

region between −180 and −90 relative to the *sdhC* start codon and binding site B between −90 and +12. Inspection of these regions revealed sequence motifs similar to the ones identified in the *acn* promoter. The relevance of these sites for RipA binding was again confirmed by mutational analysis (supplemental Fig. S1). Based on the four RipA binding sites identified upstream of *acn* and *sdhC*, the other RipA target promoters were searched for motifs similar to G(A/T)GCGN5(T/C)GAC, and the relevance of putative motifs was subsequently tested by changing three adjacent nucleotides within the motif. In this way, two binding sites were identified upstream of *narK* and *pta*, three upstream of *katA*, and one upstream of *leuC* and *catA*. Fig. 7 gives an overview of all identified RipA binding sites, their position relative to the respective start codon, and their orientation. From the alignment of the 13 binding sites, the RipA consensus motif RRGCGN$_4$RYGAC was derived. From the 13 motifs, two were present in inverted orientation (acn-B and pta-A). The distance between neighboring RipA binding sites varied between 57 and 339 bp.

Regulation of ripA Expression by DtxR—As shown previously (2), expression of *ripA* followed the same pattern as that of typical iron acquisition genes (*i.e.* its mRNA level was always increased under iron-limiting conditions). In *Corynebacterium diphtheriae*, DtxR in complex with iron represses expression of the iron starvation proteins under iron excess but is inactivated under iron limitation (28). *C. glutamicum* contains a protein with 72% sequence identity to *C. diphtheriae* DtxR (encoded by NCgl1845), and the *C. glutamicum* homolog was previously shown to repress the *tox* promoter from *C. diphtheriae* in an iron-dependent manner (29). It was therefore tempting to speculate that expression of *ripA* is repressed under iron excess by DtxR and derepressed under iron starvation. A 19-bp consensus operator of DtxR from *C. diphtheriae* has been defined as TWAGGTTAGSCTAACCTWA (30). Inspection of the *C. glutamicum ripA* promoter region revealed a sequence motif (*i.e.* TGAGGTTAGCGTAACCTAC) that differs in only three positions from the consensus binding site and ends 32 bp upstream of the *ripA* start codon. In order to test whether this motif is a DtxR binding site, the DtxR protein from *C. glutamicum* was overproduced in *E. coli* and isolated by means of a carboxyl-terminal histidine tag (Fig. 2). Gel shift analysis revealed that the purified DtxR protein bound to the *ripA* promoter region (Fig. 8). A partial shift was

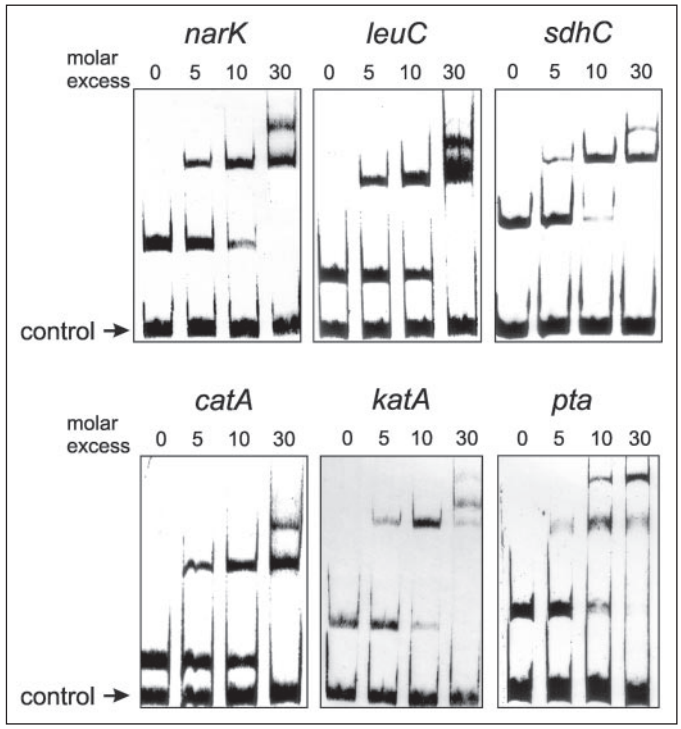

FIGURE 6. **Binding of RipA to the promoter regions of *narK*, *leuC*, *sdhC*, *catA*, *katA*, and *pta*.** DNA fragments (400–600 bp) covering the promoter regions of *narK* (13 nM), *leuC* (13 nM), *sdhC* (10 nM), *catA* (17 nM), *katA* (13 nM), and *pta* (9 nM) were incubated for 30 min at room temperature with a 5-, 10-, or 30-fold excess of purified RipA protein before separation by native polyacrylamide gel electrophoresis (10%) and staining with SybrGreen I. DNA fragments (200–350 bp) covering the promoter regions of *clpC* or *ripA* served as negative controls.

observed at a 20-fold molar excess (protein/DNA), whereas a 100-fold molar excess was required for a complete shift. Binding of DtxR to the *ripA* promoter was strictly dependent on the presence of divalent cations (*e.g.* Mn^{2+}) (data not shown). As a negative control, the promoter region of *acn* was used, which was not shifted. These results clearly support a regulation of *ripA* expression by DtxR.

RipA binding site	Sequence	Position	Orientation
acn-A	AA GAGCGGGAACCGAC TT	-312.5	+
acn-B	AC GTGCGTGATGTGAC TT	-255.5	-
sdhC-A	AT GAGCGTCAAACGAC AA	-138.5	+
sdhC-B	GG GAGCGCCCCGTGAC TG	-57.5	+
narK-A	TA AAGTGAATTACGAC AC	-148.5	+
narK-B	AG AGGCATCACGTGAC AC	-2.5	+
pta-A	AA GCGCGCAGCGTGAC AA	-268.5	-
pta-B	AC AAGCCTGAAGTGTC AT	-2.5	+
katA-A	GG GGGCGTGCCATGTC GT	-485.5	+
katA-B	AG GAGCGCGCTGCGAA GC	-410.5	+
katA-C	GG TGGCGCGAAGTGAC AT	-71.5	+
leuC-A	TT GGGCGGGACGTGAC AT	-98.5	+
catA-A	TG AAGCGGTGTGTGAC AT	-342.5	+
Consensus	dn RRGCGNNNNRYGAC wn		

FIGURE 7. **Overview on RipA binding sites.** The 13 RipA binding sites identified in this work were aligned. The position of the center of the binding sites relative to the translation start site is given by the *numbers* in the *position column*, and the orientation of the binding sites is indicated by *plus* and *minus signs*. The designations *A*, *B*, and *C* of the binding sites were assigned according to the distance to the translation start site, with the A sites located most distantly. In the derived consensus sequence, single residues are indicated when they occur in at least 10 binding sites. The first two and the last two bases shown are probably not essential for binding, since mutation of these sites did not inhibit RipA binding in the case of acn-A, acn-B, sdhC-A and sdh-B. The bases interfering with RipA binding in the case of the *acn* and *sdhC* regions are shown in Figs. 5 and S1, respectively. The relevance of the other binding sites was confirmed by showing that mutation of three consecutive bases inhibited binding of RipA to the fragment containing the proposed binding site. The bases mutated were GAC for narK-A, GGC for narK-B, GCG for pta-A, GTC for pta-B, GCG for katA-A, GAG for katA-B, GCG for katA-C, GCG for leuC-A, and GCG for catA-A.

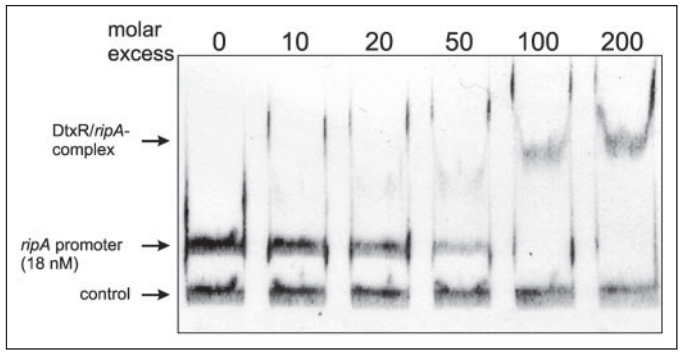

FIGURE 8. **Binding of DtxR to the *ripA* promoter region.** Different concentrations of purified DtxR protein (10–200-fold molar excess) were incubated with 18 nM of a 320-bp DNA fragment covering the *ripA* promoter region (−230 to +70 relative to the translation start site), including a putative DtxR binding site (TGAGGTTAGCGTAACCTAC). A 200-bp fragment covering the promoter region of *acn* served as a negative control. The samples were separated by native polyacrylamide gel electrophoresis, and DNA was stained with SybrGreen I.

DISCUSSION

Iron is a critical element for bacteria, being essential as a co-factor in a multitude of enzymes, poorly soluble and dangerous, by catalyzing the formation of reactive oxygen species (25). Therefore, most cells have sophisticated regulatory systems to ensure a sufficient supply of iron but to avoid high levels of free Fe^{2+}, the form responsible for hydroxyl radical production via the Fenton reaction (31). In many Gram-negative and low GC Gram-positive bacteria, the Fur protein is the central regulator of iron regulation (32, 33), whereas in many high GC Gram-positive genera (*e.g. Corynebacterium*, *Mycobacterium*, *Rhodococcus*, or *Streptomyces*), DtxR and homologous proteins are the key regulators in iron metabolism (28, 34). Under iron excess, DtxR in complex with its co-repressor Fe^{2+} represses its target genes, in particular uptake systems for iron siderophores, heme, or other iron sources. When iron becomes limiting, Fe^{2+} dissociates from DtxR, and apo-DtxR dissociates from its target promoters. The DtxR protein was first identified in *C. diphtheriae*, where it regulates the expression of the diphtheria toxin gene carried by corynebacteriophage β. In this work, we have unraveled a completely new aspect of DtxR (*i.e.* its influence on the expression of several prominent iron-containing proteins via the AraC-type regulator RipA).

The involvement of RipA in iron-dependent regulation was suggested by recent microarray experiments in which the *ripA* mRNA level was always found to be increased under iron limitation, similar to a multitude of iron acquisition genes (2). In our present study, transcriptome comparisons of a Δ*ripA* mutant and the wild type revealed seven operons whose mRNA level was increased in the Δ*ripA* mutant under iron limitation, but not under iron excess (*i.e.* those encoding aconitase (*acn*), isopropylmalate dehydratase (*leuCD*), succinate dehydrogenase (*sdhCAB*), nitrate/nitrite transporter and nitrate reductase (*narKGHJI*), catechol 1,2-dioxygenase (*catA*), phosphotransacetylase (*pta*), and catalase (*katA*)). The hypothesis that RipA functions as a repressor of these operons was supported by gel shift assays showing that purified RipA binds to the seven corresponding promoter upstream regions. In all cases, at least two RipA-DNA complexes of distinct mobility were identified in the gel shift experiments, suggesting the presence of at least two RipA binding sites. Using subfragments and mutational analysis, the binding sites upstream of *acn* and *sdhCAB* were identified and used to search for similar sequences in the other target promoters. Subsequently, mutational analysis led to the identification of three binding sites upstream of *katA* and of two binding sites upstream of *narKGHJI* and *pta*, whereas in the case of *catA* and *leuCD* only one of the binding sites could be identified up to now. Alignment of the corresponding sequences revealed a minimal consensus sequence of the type RRGCGN$_4$RYGAC. AraC-type regulators (35, 36) contain two adjacent helix-turn-helix (HTH)[3] motifs, which in the case of MarA insert in two adjacent segments of the major groove of the *mar* promoter (37). Thus, one might speculate that one HTH motif of RipA interacts with the conserved RRGCG motif and the adjacent HTH with the RYGAC motif.

Whereas the vast majority of AraC-type regulators investigated to date function as transcriptional activators (35, 36), the results presented here indicate that RipA predominantly acts as a transcriptional repressor. Repression is usually accomplished by binding of the regulator between the −35 and −10 regions of the promoter and blocking access of RNA polymerase. From the RipA target operons identified in this work, transcriptional start sites have been determined for *acn* (located 113 bp (TS2) and 110 bp (TS1) upstream of the start codon (2)) and for *pta* (located 158 bp (TS2) and 46 bp (TS1) upstream of the initiation codon (38)). In the case of *acn*, the two identified RipA binding sites are centered at −203.5 and −146.5 with respect to TS2. Since these sites are far upstream of the RNA polymerase binding site, the question arises of how RipA represses *acn* expression. One possibility is the presence of one or more additional binding sites that we have not yet identified. A weak third RipA-*acn* complex that was observed at high RipA concentrations (Fig. 4*B*) supports this suggestion. A promising RipA binding motif is located immediately downstream of the *acn* start codon (GAGCTCACTGTGAC). However, fragment 4 in Fig. 4*A*, which contains this motif, was not shifted by RipA, at least under the conditions used in the experiment. Possibly, this site can only be occupied after previous binding to one of the other sites or under different conditions. Another possibility could be that an additional protein is involved whose binding is influenced by the presence of RipA. In the case of *pta*, the identified RipA binding sites are centered at −111.5 and +156.5 with respect to TS2, with the second binding site overlapping the *pta*

[3] The abbreviation used is: HTH, helix-turn-helix.

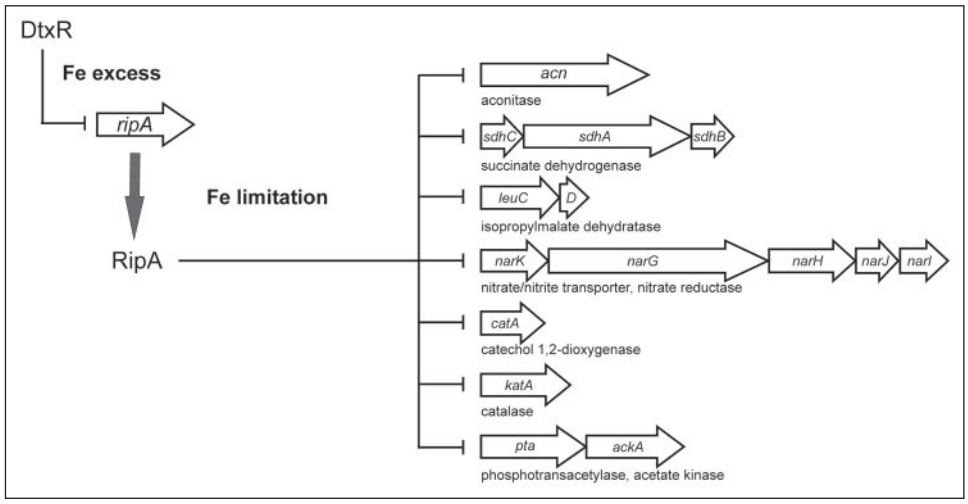

FIGURE 9. **Model of the regulatory cascade involving DtxR and RipA and organization of the RipA target genes.** Under iron excess, DtxR represses the expression of *ripA*. Under iron limitation, DtxR repression is relieved, and RipA protein is synthesized and partially represses expression of its target genes, which encode iron-containing proteins, except for *narK*, *pta*, and *ackA*. In this way, intracellular iron usage is modulated and supplements mechanisms for iron uptake that are directly regulated by DtxR.

start codon. In this case, direct inhibition of transcription by RipA can be envisaged. For *narKGHJI*, the RipA binding sites are centered at −149.5 and −2.5 with respect to the *narK* start codon. As in the case of *pta*, the second site very likely interferes with transcription of the *nar* operon. In the case of *sdhCAB*, *katA*, *catA*, and *leuCD*, no predictions can be made on the mechanism of repression yet. The presence of at least two binding sites in each RipA target promoter and the large and varying distances between these binding sites might suggest that DNA looping is involved in the mechanism of action of RipA, as reported, for example, for the AraC-type regulators AraC (39) and MelR (40).

Except for the nitrate/nitrite transporter NarK and presumably phosphotransacetylase, all of the enzymes repressed by RipA contain iron; aconitase and isopropylmalate dehydratase possess one iron-sulfur cluster, succinate dehydrogenase probably harbors three iron-sulfur clusters and two hemes (24), nitrate reductase presumably contains four iron sulfur-clusters and two hemes (24), catalase contains heme,[4] and catechol 1,2-dioxygenase contains one non-heme iron (41). Therefore, it is obvious to assume that a major function of RipA is to reduce the synthesis of iron proteins under iron-limiting conditions, thus reducing the cell's iron demand and preventing the formation of inactive apoenzymes lacking iron. In agreement with such a function, the mRNA levels of *acn*, *leuCD*, *sdhCAB*, *narKGHJI*, *catA*, *pta*, and *katA* were decreased under iron limitation compared with iron excess, both in the wild type and in the Δ*acnR* mutant (2). Whereas repression of the non-iron protein NarK can be explained by co-transcription with the nitrate reductase structural genes, the inclusion of phosphotransacetylase in the RipA regulon must have other reasons. A dependence on iron has only been described for the enzyme of *Clostridium acidiurici* (42), whereas phosphotransacetylase from other species apparently does not require iron. Phosphotransacetylase catalyzes the reversible conversion of acetylphosphate and acetyl-CoA and, in concert with acetate kinase, is involved in the catabolism of acetate (38) as well as in the formation of acetate from acetyl-CoA. *C. glutamicum*, in contrast to *E. coli*, usually does not form acetate as a product of aerobic overflow metabolism, and therefore the primary function of phosphotransacetylase in this species appears to be in acetate utilization. Since acetate catabolism involves a 2–3-fold higher carbon flux through the citric acid cycle compared with growth on glucose (43), repression of *pta* by RipA may serve to reduce acetate utilization under iron limitation and thus to prevent an increased citric acid cycle flux, which cannot be maintained if aconitase and succinate dehydrogenase are repressed at the same time.

A regulatory cascade with an analogous function to that of DtxR and RipA in *Corynebacterium* is found in *E. coli*. Here the role of DtxR is fulfilled by Fur, whereas the small RNA RyhB plays a function similar to that of RipA (44). Expression of *ryhB* is repressed by Fur under iron excess and increases under iron limitation. RyhB acts as an antisense RNA and inhibits translation of the mRNAs encoding succinate dehydrogenase (*sdhCDAB*), aconitase A (*acnA*), fumarase A (*fumA*), ferritin (*ftnA*), bacterioferritin (*bfr*), and superoxide dismutase B (*sodB*). Although the spectrum of target genes regulated by RipA and RyhB only partially overlaps, it is remarkable that both involve the iron-containing proteins of the citric acid cycle (the only fumarase of *C. glutamicum* belongs to the type II fumarases and does not contain iron).

A search for the distribution of RipA revealed that homologous proteins are only present in *Corynebacterium efficiens* (CE1047; 70.1% sequence identity) and *C. diphtheriae* (DIP0922; 51.5% sequence identity), but not in *Corynebacterium jeikeium* (45) and other high GC gram positives (*e.g.* the genera *Mycobacterium* or *Streptomyces*). The *C. efficiens ripA* gene, as annotated in the genome sequence (46), encodes a protein of 400 amino acids. We prefer an ATG start codon that is located 68 codons downstream of the annotated GTG start codon, because the derived protein has a length comparable with the RipA proteins from *C. glutamicum* and *C. diphtheriae* (supplemental Fig. S2) and because a well conserved DtxR binding site (TGAGGTTAGCGTAACCTAC) deviating in only two positions from the consensus sequence (30) ends 40 bp upstream of the *ripA* ATG start codon proposed here (164 bp downstream of the annotated GTG start codon). In *C. diphtheriae*, the annotated genome sequence from strain NCTC13129 predicts that the *ripA* homologous gene DIP0922 encodes a protein of 335 amino acid residues (47). Inspection of the corresponding upstream sequence revealed a putative DtxR binding site (CGAGCAAGGAGTAACCTTA) ending 87 bp upstream of the proposed start codon, which, however, differed in eight positions from the consensus sequence and thus is quite speculative. Interestingly, Lee *et al.* (48) previously identified a DtxR-regulated gene region designated IRP3 from *C. diphtheriae* strain C7, which is equivalent to the one described above. The DtxR binding site they identified experimentally by DNase I footprinting (TTAGGTGAGACGCACCCAT) is located upstream of an open reading frame encoding a 124-amino acid polypeptide showing high identity to regions of *C. diphtheriae* RipA (data not shown). The IRP3 DtxR binding site starts 267 bp downstream of the proposed start codon of

[4] M. Bott and M. Wingens, unpublished data.

DIP0922. Further studies are required to determine the relevance of the strain differences and the functionality of the putative DtxR binding site upstream of DIP0922.

The discovery of RipA as a repressor of iron proteins and its own repression by DtxR have unraveled a new aspect of the regulatory network controlling iron metabolism in *Corynebacterium* (Fig. 9). Aspects that have to be addressed in future work are the mechanism(s) of repression by RipA and the mechanism of RipA inactivation after a shift from iron limitation to iron excess. This will probably require an understanding of the function of the N- and C-terminal domains that show no homology to other proteins.

Acknowledgments—We thank Hermann Sahm for continuous support and Volker Wendisch for stimulating discussions in the initial phase of this project and for establishing the DNA chip technique in our institute.

REFERENCES

1. Eggeling, L., and Bott, M. (eds) (2005) *Handbook of Corynebacterium glutamicum*, CRC Press, Taylor & Francis Group, Boca Raton, FL
2. Krug, A., Wendisch, V. F., and Bott, M. (2005) *J. Biol. Chem.* **280,** 585–595
3. Kinoshita, S., Udaka, S., and Shimono, M. (1957) *J. Gen. Appl. Microbiol.* **3,** 193–205
4. Sambrook, J., Fritsch, E. F., and Maniatis, T. (1989) *Molecular Cloning: A Laboratory Manual*, Cold Spring Harbor Laboratory, Cold Spring Harbor, NY
5. Keilhauer, C., Eggeling, L., and Sahm, H. (1993) *J. Bacteriol.* **175,** 5595–5603
6. Studier, F. W., and Moffatt, B. A. (1986) *J. Mol. Biol.* **189,** 113–130
7. Eikmanns, B. J., Thum-Schmitz, N., Eggeling, L., Luedtke, K. U., and Sahm, H. (1994) *Microbiology* **140,** 1817–1828
8. Hanahan, D. (1985) in *DNA Cloning* (Glover, D. M., ed) Vol. 1, pp. 109–135, IRL Press, Oxford, UK
9. van der Rest, M. E., Lange, C., and Molenaar, D. (1999) *Appl. Microbiol. Biotechnol.* **52,** 541–545
10. Niebisch, A., and Bott, M. (2001) *Arch. Microbiol.* **175,** 282–294
11. Schäfer, A., Tauch, A., Jäger, W., Kalinowski, J., Thierbach, G., and Pühler, A. (1994) *Gene* (*Amst.*) **145,** 69–73
12. Cremer, J., Eggeling, L., and Sahm, H. (1990) *Mol. Gen. Genet.* **220,** 478–480
13. Skerra, A., and Schmidt, T. G. (2000) *Methods Enzymol.* **326,** 271–304
14. Engels, S., Schweitzer, J. E., Ludwig, C., Bott, M., and Schaffer, S. (2004) *Mol. Microbiol.* **52,** 285–302
15. Möker, N., Brocker, M., Schaffer, S., Krämer, R., Morbach, S., and Bott, M. (2004) *Mol. Microbiol.* **54,** 420–438
16. Wendisch, V. F. (2003) *J. Biotechnol.* **104,** 273–285
17. Lange, C., Rittmann, D., Wendisch, V. F., Bott, M., and Sahm, H. (2003) *Appl. Environ. Microbiol.* **69,** 2521–2532
18. Polen, T., and Wendisch, V. F. (2004) *Appl. Biochem. Biotech.* **118,** 215–232
19. Ishige, T., Krause, M., Bott, M., Wendisch, V. F., and Sahm, H. (2003) *J. Bacteriol.* **185,** 4519–4529
20. Henson, C. P., and Cleland, W. W. (1967) *J. Biol. Chem.* **242,** 3833-&
21. Bateman, A., Coin, L., Durbin, R., Finn, R. D., Hollich, V., Griffiths-Jones, S., Khanna, A., Marshall, M., Moxon, S., Sonnhammer, E. L. L., Studholme, D. J., Yeats, C., and Eddy, S. R. (2004) *Nucleic Acids Res.* **32,** D138–D141
22. Falquet, L., Pagni, M., Bucher, P., Hulo, N., Sigrist, C. J. A., Hofmann, K., and Bairoch, A. (2002) *Nucleic Acids Res.* **30,** 235–238
23. Reinscheid, D. J., Schnicke, S., Rittmann, D., Zahnow, U., Sahm, H., and Eikmanns, B. J. (1999) *Microbiology* **145,** 503–513
24. Bott, M., and Niebisch, A. (2003) *J. Biotechnol.* **104,** 129–153
25. Andrews, S. C., Robinson, A. K., and Rodriguez-Quinones, F. (2003) *FEMS Microbiol. Rev.* **27,** 215–237
26. Smith, J. L. (2004) *Crit. Rev. Microbiol.* **30,** 173–185
27. Costa-Riu, N., Maier, E., Burkovski, A., Kramer, R., Lottspeich, F., and Benz, R. (2003) *Mol. Microbiol.* **50,** 1295–1308
28. Tao, X., Schiering, N., Zeng, H. Y., Ringe, D., and Murphy, J. R. (1994) *Mol. Microbiol.* **14,** 191–197
29. Oguiza, J. A., Tao, X., Marcos, A. T., Martin, J. F., and Murphy, J. R. (1995) *J. Bacteriol.* **177,** 465–467
30. Tao, X., and Murphy, J. R. (1994) *Proc. Natl. Acad. Sci. U. S. A.* **91,** 9646–9650
31. Pierre, J. L., and Fontecave, M. (1999) *Biometals* **12,** 195–199
32. Hantke, K. (2001) *Curr. Opin. Microbiol.* **4,** 172–177
33. Escolar, L., Perez-Martin, J., and De Lorenzo, V. (1999) *J. Bacteriol.* **181,** 6223–6229
34. Rodriguez, G. M., and Smith, I. (2003) *Mol. Microbiol.* **47,** 1485–1494
35. Gallegos, M. T., Schleif, R., Bairoch, A., Hofmann, K., and Ramos, J. L. (1997) *Microbiol. Mol. Biol. Rev.* **61,** 393-&
36. Martin, R. G., and Rosner, J. L. (2001) *Curr. Opin. Microbiol.* **4,** 132–137
37. Rhee, S., Martin, R. G., Rosner, J. L., and Davies, D. R. (1998) *Proc. Natl. Acad. Sci. U. S. A.* **95,** 10413–10418
38. Gerstmeir, R., Wendisch, V. F., Schnicke, S., Ruan, H., Farwick, M., Reinscheid, D., and Eikmanns, B. J. (2003) *J. Biotechnol.* **104,** 99–122
39. Lobell, R. B., and Schleif, R. F. (1990) *Science* **250,** 528–532
40. Wade, J. T., Belyaeva, T. A., Hyde, E. I., and Busby, S. J. W. (2000) *Mol. Microbiol.* **36,** 223–229
41. Shen, X. H., Liu, Z. P., and Liu, S. J. (2004) *Biotechnol. Lett.* **26,** 575–580
42. Robinson, J. R., and Sagers, R. D. (1972) *J. Bacteriol.* **112,** 465–473
43. Wendisch, V. F., De Graaf, A. A., Sahm, H., and Eikmanns, B. J. (2000) *J. Bacteriol.* **182,** 3088–3096
44. Masse, E., and Gottesman, S. (2002) *Proc. Natl. Acad. Sci. U. S. A.* **99,** 4620–4625
45. Tauch, A., Kaiser, O., Hain, T., Goesmann, A., Weisshaar, B., Albersmeier, A., Bekel, T., Bischoff, N., Brune, I., Chakraborty, T., Kalinowski, J., Meyer, F., Rupp, O., Schneiker, S., Viehoever, P., and Puhler, A. (2005) *J. Bacteriol.* **187,** 4671–4682
46. Nishio, Y., Nakamura, Y., Kawarabayasi, Y., Usuda, Y., Kimura, E., Sugimoto, S., Matsui, K., Yamagishi, A., Kikuchi, H., Ikeo, K., and Gojobori, T. (2003) *Genome Res.* **13,** 1572–1579
47. Cerdeno-Tarraga, A. M., Efstratiou, A., Dover, L. G., Holden, M. T. G., Pallen, M., Bentley, S. D., Besra, G. S., Churcher, C., James, K. D., De Zoysa, A., Chillingworth, T., Cronin, A., Dowd, L., Feltwell, T., Hamlin, N., Holroyd, S., Jagels, K., Moule, S., Quail, M. A., Rabbinowitsch, E., Rutherford, K. M., Thomson, N. R., Unwin, L., Whitehead, S., Barrell, B. G., and Parkhill, J. (2003) *Nucleic Acids Res.* **31,** 6516–6523
48. Lee, J. H., Wang, T., Ault, K., Liu, J., Schmitt, M. P., and Holmes, R. K. (1997) *Infect. Immun.* **65,** 4273–4280